Mechanism of Adenylate Kinase. The "Essential Lysine" Helps To Orient the Phosphates and the Active Site Residues to Proper Conformations†

In-Ja L. Byeon, Zhengtao Shi, and Ming-Daw Tsai*,‡

Department of Chemistry, The Ohio State University, Columbus, Ohio 43210

Received September 9, 1994; Revised Manuscript Received December 12, 1994⊗

ABSTRACT: Although how Lys21 interacts with the substrate MgATP of muscle adenylate kinase (AK) can now be deduced from the crystal structure of *Escherichia coli* AK·MgAP$_5$A [P^1,P^5-bis(5′-adenosyl) pentaphosphate] [Müller, C. W., & Schulz, G. E. (1992) *J. Mol. Biol. 224,* 159−177], its contribution to catalysis has not yet been demonstrated by functional studies since the proton NMR of the K21M mutant was shown to be perturbed significantly [Tian, G., Yan, H., Jiang, R.-T., Kishi, F., Nakazawa, A., & Tsai, M.-D. (1990) *Biochemistry 29,* 4296−4304]. We therefore undertook further structural and functional analyses of a conservative mutant K21R and a nonconservative mutant K21A. In addition to kinetic analyses, the structures of the mutants were analyzed by one- and two-dimensional proton NMR spectroscopy and {^{1}H, ^{15}N} heteronuclear multiple-quantum coherence (HMQC) experiments. Detailed assignments were performed in reference to the total backbone assignments of the WT AK·MgAP$_5$A complex [Byeon, I.-J. L., Yan, H., Edison, A. S., Mooberry, E. S., Abildgaard, F., Markley, J. L., & Tsai, M.-D. (1993) *Biochemistry 32,* 12508−12521]. The analysis showed that the residues located near the active site (Gly15, Thr23, Arg97, Gln101, Arg128, Arg132, Asp140, Asp141, and Tyr153) exhibit greater changes in ^{1}H−^{15}N chemical shifts. Finally, two-dimensional ^{31}P−^{31}P COSY experiments were used to examine the effects of the lysine side chain on the phosphate groups in the bound AP$_5$A. Our data have led to the following conclusions independent of the crystal structure: (i) Because the perturbations in the conformation of the mutants are not global and are mainly localized at active site residues and Tyr153, the side chain of Lys21 can be concluded to stabilize the transition state in the catalysis of AK by up to 7 kcal/mol on the basis of the 10^5-fold decreases in the k_{cat}/K_m of mutants. (ii) The results of ^{31}P NMR analyses suggest that Lys21 functions by orienting the triphosphate chain of MgATP to a proper conformation required for catalysis. (iii) The interaction between Lys21 and the phosphate chain in turn dictates the interactions between the substrates and the active site residues. In the K21R·MgATP complex, the NH chemical shifts of many of the active site residues are perturbed. (iv) The catalytic functions of Lys21 cannot be replaced by a conservative residue arginine. In addition, since K21A and K21R behave similarly, the catalytic function of Lys21 should not be merely a charge effect.

Most, if not all, kinases have an "invariant lysine". In the case of adenylate kinase (AK)[1] from chicken muscle, this invariant lysine is Lys21 located at the phosphate-binding loop (P-loop) (Schulz et al., 1986; Saraste et al., 1990). The functional importance of this lysine has been demonstrated by the fact that chemical modification of this lysine leads to a dramatic loss of catalytic activity and that the modification and inactivation can often be protected by ATP or MgATP (Tagaya et al., 1987; Yagami et al., 1988). The 1.9 Å crystal structure of the *Escherichia coli* AK·MgAP$_5$A complex shows that this lysine (residue 13 in the *E. coli* AK) forms hydrogen bonds with the β- and γ-phosphate groups of the ATP moiety of MgAP$_5$A (Müller & Schulz, 1992). Similar structures have also been observed in the crystal structure of *ras* p21 (Wittinghofer & Pai, 1991), which has often been compared with adenylate kinase in terms of the mode of substrate binding.

Why are we still interested in the functional study of this residue now that the specific interaction between Lys21 and the bisubstrate analog inhibitor MgAP$_5$A has been revealed by the crystal structures? Our goal is twofold: to understand the quantitative energetic contribution of the specific interactions to catalysis and to understand *how* such interactions affect catalysis at the structural level, beyond what can be learned from crystal structures. In an earlier effort toward this goal, we have constructed the K21M mutant and characterized its structural and functional properties (Tian et al., 1990). The k_{cat} of this mutant was found to decrease by a factor of 4×10^4, which suggested the importance of this residue in catalysis. However, 1D proton NMR analysis suggested that the conformation of the K21M mutant has been globally perturbed. We therefore concluded that Lys21

† This work was supported by a grant from National Institutes of Health (GM43268). This study made use of Bruker MSL-300, AM-500, and DMX-600 NMR spectrometers at The Ohio State University funded by NIH Grants RR01458 and RR08299 and NSF Grant BIR-9221639. This is paper 18 in the series Mechanism of Adenylate Kinase. For paper 17, see Tsai et al. (1994).

‡ Also a member of the Department of Biochemistry.

⊗ Abstract published in *Advance ACS Abstracts,* February 15, 1995.

[1] Abbreviations: ADP, adenosine 5′-diphosphate; AK, adenylate kinase; AMP, adenosine 5′-monophosphate; AMPPNP, 5′-adenylyl imidodiphosphate; AP$_5$A, P^1,P^5-bis(5′-adenosyl) pentaphosphate; ATP, adenosine 5′-triphosphate; COSY, correlation spectroscopy; DTT, dithiothreitol; EDTA, ethylenediaminetetraacetate; FPLC, fast-performance liquid chromatography; GARP, globally optimized alterating phase rectangular pulse; GB, Gaussian broadening; HMQC, heteronuclear multiple-quantum coherence spectroscopy; LB, line broadening; NMR, nuclear magnetic resonance; NOE, nuclear Overhauser effect; NOESY, nuclear Overhauser enhanced spectroscopy; PAGE, polyacrylamide gel electrophoresis; pH*, glass electrode pH reading uncorrected for deuterium isotope effects; SDS, sodium dodecyl sulfate; Tris, 2-amino-2-(hydroxymethyl)-1,3-propanediol; WT, wild type; 1D, one dimensional; 2D, two dimensional.

0006-2960/95/0434-3172$09.00/0

plays a structural role possibly by stabilizing the P-loop and that its specific functional role in catalysis remains to be established. The K13Q mutant of *E. coli* AK (Lys13 corresponds to Lys21 in muscle AK) also displayed a large decrease in k_{cat} and an appreciable perturbation in 1D proton NMR spectra (Reinstein et al., 1990). However, the authors proposed as a working hypothesis that the main function of the side chain of this lysine is to stabilize the pentacovalent transition state of the transferring phosphoryl group during the catalytic reaction.

In a strict sense, the quantitative contribution of Lys21 to catalysis is still unresolved since the kinetic data cannot be interpreted quantitatively due to perturbations in the proton NMR property. Even if the kinetic data can be interpreted with confidence, kinetic results do not provide structural information. We therefore undertook further structural and functional analyses of a conservative mutant K21R and a nonconservative mutant K21A. Our system is chicken muscle AK overexpressed in *E. coli*.[2] At first we showed that the k_{cat} values of both mutants are comparable to that of K21M, reaffirming the potential importance of Lys21 in catalysis. The conformations of the mutants and their complexes with the bisubstrate analog $MgAP_5A$ were then analyzed in detail by NOESY and {^1H, ^{15}N} HMQC experiments. The availability of the total backbone assignment of the WT AK complexed with $MgAP_5A$ (Byeon et al., 1993) has allowed us to identify the residues undergoing larger shifts. The results indicate that the residues with greater changes in chemical shifts are mostly located near the active site. The most shifted aromatic side chain, Tyr153, is likely to be involved in substrate-induced conformational changes. Finally, ^{31}P NMR analyses provided evidence that the main function of the interaction between Lys21 and the substrates is to help to orient the phosphate chain to a proper conformation for catalysis. The results led to interpretation of the structural and functional roles of Lys21 in molecular detail.

MATERIALS AND METHODS

Materials. The K21R mutant was generated by degenerate oligonucleotides CGGCTCAGGGC(A/G)GGGGACGCAA whereas K21A was generated by a single oligonucleotide CGGCTCAGGGGCGGGGACGCAA. Y153F and Y153L were generated by degenerate oligonucleotides CTTGGAGACGTT(T/G)TACAAGGCTA. The oligonucleotides were synthesized at the Biochemical Instrument Center of The Ohio State University. DNA sequencing and mutagenesis kits were purchased from United States Biochemicals and Amersham, respectively. Phosphocellulose-11 and Sephadex G-100 resins were purchased from Whatman and Sigma, respectively. Affi-Gel Blue and phenyl-Sepharose CL-4B resins were obtained from Bio-Rad and Pharmacia, respectively. Perdeuterated Tris and D_2O were purchased from MSD Isotopes. $(^{15}NH_4)_2SO_4$ was purchased from either Cambridge Isotope Laboratory or Isotec Inc. ADP, AMP, AP_5A, ATP, coupling enzymes, and other reagents were obtained from Sigma.

Construction and Purification of Mutant Enzymes. The mutants K21R, K21A, Y153F, and Y153L were constructed by using the mutagenesis kit from Amersham and the procedure described in its manual. The full-length AK gene was sequenced by the dideoxynucleotide terminating method to screen and verify the designed mutations. The method used to purify the mutants K21R, Y153F, and Y153L was essentially the same as that described by Tian et al. (1988) for WT AK. It is worth noting that the yield of Y153L is much lower than that of other AK mutants due to its structural instability. Since the mutant K21A did not bind well to the phosphocellulose-11 column, an Affi-Gel Blue column to which the mutant exhibited high affinity was used for its purification. The bound mutant was eluted from the column using a 0−400 mM NaCl gradient. Fractions containing K21A were collected and further purified by a G-100 gel chromatography. Although the purity of the enzyme, examined by SDS−PAGE with silver staining on a PhastSystem, was greater than 95%, it was contaminated with *E. coli* AK. The contamination was eliminated by a phenyl-Sepharose CL-4B column chromatography: the column (a bed volume of 10 mL) was connected to an FPLC system from Pharmacia and equilibrated with at least 20× bed volumes of buffer A [30 mM Tris, 1 mM DTT, and 0.8 M $(NH_4)_2SO_4$, pH 7.5 at room temperature]. About 20 mg of K21A dissolved in 0.2 mL of buffer A was loaded onto the column. The column was then washed with buffer A at a flow rate of 1 mL/min. K21A was eluted off during the washing step. The pooled K21A sample was dialyzed and lyophilized in the same way as for WT AK (Tian et al., 1988).

Uniformly ^{15}N-labeled AK samples were prepared by growing the bacteria in the M9 minimum media with $(^{15}NH_4)_2SO_4$ as the sole nitrogen source.

Steady-State Kinetics. The kinetic experiments were carried out at 30 °C and pH 8.0 by monitoring ADP formation with pyruvate kinase/lactate dehydrogenase as the coupling system (Rhoads & Lowenstein, 1968). The values of k_{cat}, K (Michaelis constant), and K_i (dissociation constant) were obtained by varying both MgATP and AMP concentrations followed by analyses according to the equation of Cleland (1986) for a random Bi-Bi system. The details have been described previously (Tian et al., 1988).

Proton NMR Methods. All proton NMR experiments were performed on a Bruker AM-500 spectrometer at 27 °C unless otherwise specified. Chemical shifts were referenced to internal sodium 3-(trimethylsilyl) propionate-*2,2,3,3-d*$_4$. NMR sample preparations were essentially the same as described by Yan et al. (1990a). All the samples were adjusted to pH* 7.5, where pH* denotes glass electrode reading uncorrected for deuterium isotope effects. The enzyme concentrations for NMR experiments were 2 mM unless otherwise specified.

Standard pulse sequences and phase cycling were used for all 2D NMR experiments: NOESY (Bodenhausen et al., 1984) and COSY (Marion & Wüthrich, 1983). All spectra were obtained in the phase-sensitive mode with time-proportional phase incrementation (Marion & Wüthrich, 1983). Spectral widths in all experiments were 6024.1 Hz in both dimensions. Generally, a 4K × (400−512) time domain matrix was recorded. In COSY experiments, the two-dimensional data matrix was multiplied with an unshifted sine bell weighting function in both dimensions. In NOESY experiments, the two-dimensional data matrix was multiplied by a shifted sine bell function (SSB1 = 12) in t_1 and by a

[2] Unless otherwise specified, the numbering system used in this paper is the conventional system for muscle AK. Although chicken muscle AK has one additional residue near the N-terminus (Kishi et al., 1986), the Met1 residue is absent in the chicken muscle AK expressed in *E. coli* (Tanizawa et al., 1987). This makes its numbering consistent with AK from other muscles.

Table 1: Comparison of Kinetic Data between WT and K21 and Y153 Mutants[a]

parameters	WT[b]	K21R	K21A	K21M[b]	Y153F	Y153L
k_{cat} (s^{-1})	650	0.11 (1.8×10^{-4})	0.043 (0.7×10^{-4})	0.015 (0.2×10^{-4})	1750	61 (0.094)
$K_{(MgATP)}$ (mM)	0.042	0.75 (18)	0.21 (5)	0.052	0.13	0.65 (16)
$K_{(AMP)}$ (mM)	0.098	1.8 (18)	0.12	0.044	0.66 (7)	2.7 (28)
$K_{i(MgATP)}$ (mM)	0.16	0.14	0.30	0.19	0.32	0.28
$K_{i(AMP)}$ (mM)	0.37	0.33	0.17	0.16	1.6	1.2
$k_{cat}/K_{(MgATP)}$ (s^{-1} M^{-1})	1.6×10^7	150 (1.0×10^{-5})	200 (1.3×10^{-5})	290 (1.9×10^{-5})	0.27×10^7 (0.17)	0.93×10^5 (0.6×10^{-3})
$k_{cat}/K_{(AMP)}$ (s^{-1} M^{-1})	0.66×10^7	61 (0.9×10^{-5})	360 (5.5×10^{-5})	340 (5.2×10^{-5})	0.55×10^7	0.22×10^5 (0.33×10^{-3})

[a] Numbers of parentheses indicate the ratios between the mutant and WT. [b] The data for WT and K21M are from Tian et al. (1990).

Gaussian function (LB = −3, GB = 0.1) in t_2. Then the data matrix was zero-filled to a 4K × 2K matrix prior to Fourier transformation. The mixing time in NOESY experiments was 120 ms.

{^1H, ^{15}N} HMQC NMR. All HMQC (Mueller, 1979) experiments were recorded on a Bruker AM-500 spectrometer equipped with a reverse probe head at 27 °C. The HMQC-NOESY experiment for the ^{15}N labeled K21R sample was carried out on a Bruker DMX-600 spectrometer equipped with a triple-resonance probe head at 27 °C. Nitrogen chemical shifts were referenced to external 1.5 M $^{15}NH_4NO_3$ in 1 M HNO_3 at 21.6 ppm (Srinvasan & Lichter, 1977). Samples contained about 2 mM AK in a 20 mM perdeuterated Tris buffer (pH 7.1, 90% ^1H_2O/10% ^2H_2O) containing 65 mM KCl, 2 mM DTT, and 0.5 mM EDTA. $MgCl_2$ (~4 mM) and AP_5A (~3 mM) were added for the sample of the AK•$MgAP_5A$ complex. Nitrogen decoupling during acquisition was obtained with a GARP (Shaka et al., 1985) sequence. Data were obtained in the phase-sensitive mode with time-proportional phase incrementation (Marion & Wüthrich, 1983). Spectral widths in proton and nitrogen dimensions were 8064 and 2427 Hz, respectively. Generally, a 2K × (200−256) time domain matrix was recorded. The data matrix was multiplied by a shifted (SSB1 = 12) sine bell function in t_1 and by a Gaussian function (LB = −3, GB = 0.05) in t_2. Then the data matrix was zero-filled to a 4K × 1K matrix prior to Fourier transformation.

Phosphorus NMR Methods. Two-dimensional phosphorus homonuclear COSY experiments were performed on a Bruker MSL-300 NMR spectrometer with a 10-mm probe head at 25 °C. Chemical shifts were referenced to external 85% H_3PO_4. Samples contained 1 mM AK and 0.9 mM AP_5A in a 20 mM perdeuterated Tris buffer (pH 7.8, 90% ^1H_2O/10% ^2H_2O) containing 65 mM KCl, 2 mM DTT, and 0.5 mM EDTA. This AK to AP_5A molar ratio assured complete binding of AP_5A and avoided any complication in data analysis arising from excess free AP_5A. Spectral widths in both dimensions were 6024 Hz. A 1K × (200−256) time domain matrix was recorded for the phosphorus COSY. The data matrix was multiplied by a shifted (SSB1 = 2) squared sine bell function in both dimensions. Then the data matrix was zero-filled to an 1K × 512 matrix prior to Fourier transformation. A total of 256 transients was acquired. Broad-band proton decoupling was achieved with the WALTZ sequence (Shaka et al., 1983).

RESULTS

Changes in Kinetic Data. The steady-state kinetic data obtained by varying both substrates are summarized in Table 1, where K and K_i represent Michaelis and dissociation constants, respectively. As shown in Table 1, the k_{cat} values of both K21R and K21A mutants decrease by a factor of 10^4, the Michaelis constants increase by a factor of 18 K21R, and the k_{cat}/K values decrease by a factor of 10^5 for both mutants. The dissociation constants $K_{i(MgATP)}$ and $K_{i(AMP)}$ calculated from the rate equation for a random Bi-Bi system (Cleland, 1986) were essentially the same as those for WT.

The kinetic data of K21R and K21A agree within an order of magnitude with those of K21M (Tian et al., 1990) and the K13Q mutant of *E. coli* AK (corresponding to the K21Q of muscle AK) (Reinstein et al., 1990). The K21M mutant showed somewhat lower k_{cat} and little change in K and K_i values, whereas the K13Q mutant showed greater increases in K values. The fact that the conservative arginine mutant behaves similarly to the other mutants suggests that the side chain of Lys21 is likely to be involved in stabilizing the transition state. However, it is important to determine whether conformational perturbations in the mutant enzymes have contributed to the observed changes in the kinetic data and, if not, "how" Lys21 interacts with the substrate(s) in structural terms. These are the goals of the following sections.

NMR Spectral Perturbations: Aromatic Side Chains. The structural perturbations of K21R and K21A mutants, in the free form and the complexes with $MgAP_5A$, were evaluated by several types of experiments: Figure 1 shows difference 1D NMR spectra between the mutants and WT, in both the free form (A and B) and the $MgAP_5A$-complexed state (C and D). These difference spectra indicate substantial, across the board changes but provide little quantitative information. A more informative comparison can be obtained from NOESY spectra of the free forms (Figure 2) and the $MgAP_5A$ complexes (Figure 3) of the enzymes. The assignments of aromatic resonances for free and $MgAP_5A$-complexed mutants were performed by comparing their NOESY and COSY (not shown) spectra with the corresponding spectra of WT whose assignments have been described in our previous publications. The results are summarized in Figure 4 and Tables 2 (free form) and 3 ($MgAP_5A$ complex). The resonances which differ by >0.02 ppm between WT and the mutants are underlined in Tables 2 and 3. As shown in Tables 2 and 3, ca. 20−30% of the resonances in each mutant complex differ from the corresponding resonances of WT by >0.02 ppm. These changes are the largest among the ca. 30 mutants of AK which have been characterized by NMR in our laboratory previously. However, the figures drop to 0−8% if the threshhold is raised to 0.1 ppm. Since chemical shifts are very sensitive to the tertiary structures of proteins, a change of 0.1 ppm is very small. Furthermore, the differences in the appearance of the NOESY spectra are mainly caused by small changes in chemical shifts. Careful

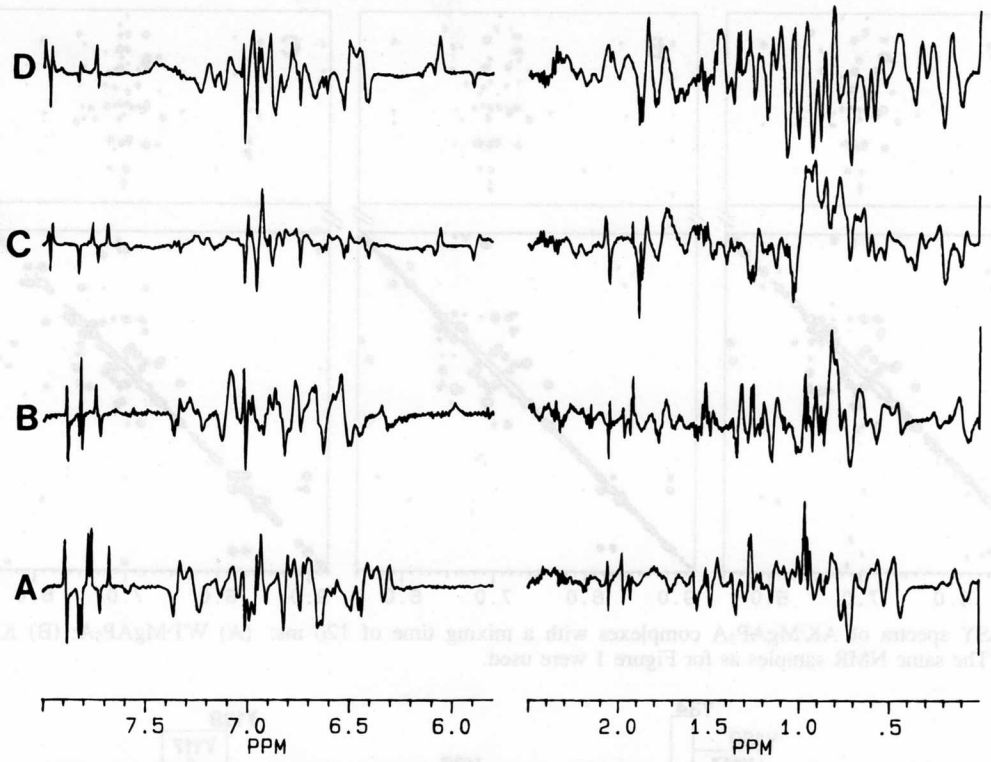

FIGURE 1: Difference proton NMR spectra at 500 MHz, 27 °C, pH* 7.5: (A) K21R − WT; (B) K21A − WT; (C) K21R·$MgAP_5A$ − WT·$MgAP_5A$; (D) K21A·$MgAP_5A$ − WT·$MgAP_5A$. The enzyme concentrations of all the samples except for the free K21A sample were 2 mM. The concentration of the free K21A was 1 mM. For the WT·$MgAP_5A$ and K21R·$MgAP_5A$ samples, [AK]:[AP_5A]:[$MgCl_2$] = 2:2.4:4.6 mM; for the K21A·$MgAP_5A$ sample, [AK]:[AP_5A]:[$MgCl_2$] = 2:3:4.6 mM.

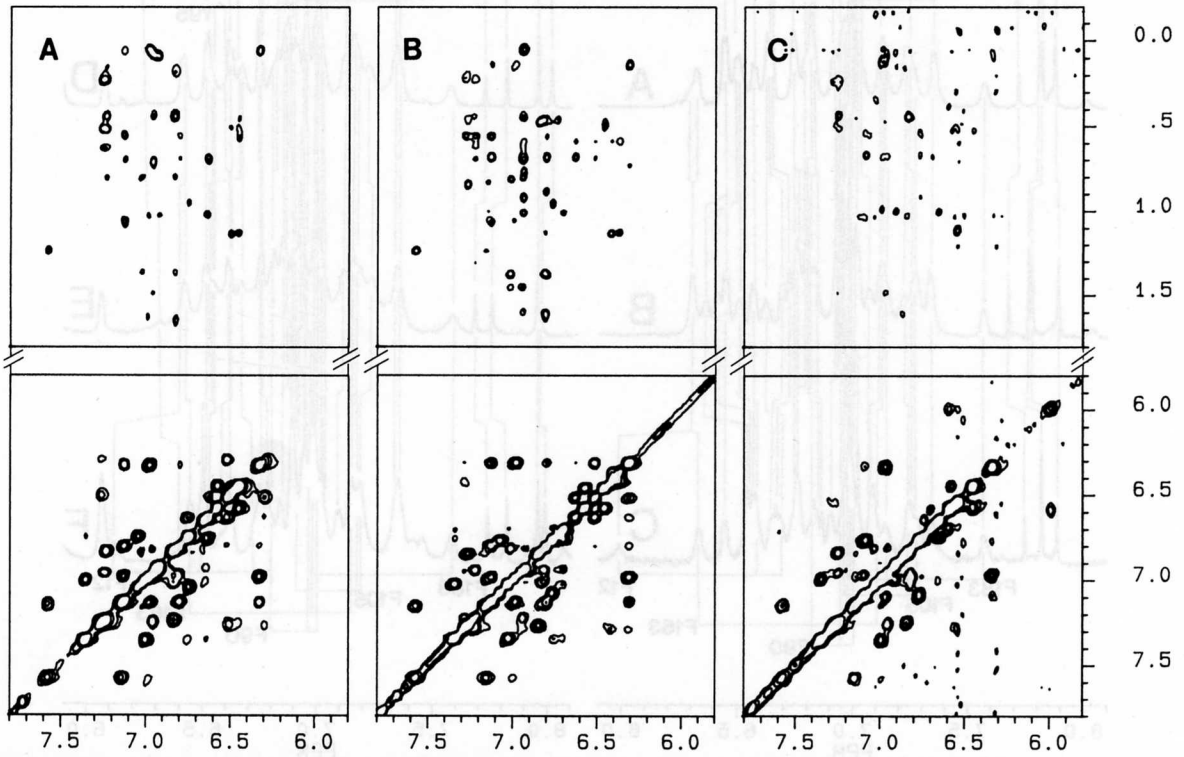

FIGURE 2: NOESY spectra of free WT (A), K21R (B), and K21A (C) with a mixing time of 120 ms. The same NMR samples as for Figure 1 were used.

examination of the spectra suggested that most of the cross-peaks identified for WT are also present in the mutants. The aliphatic side chains have not been assigned for the mutants; a qualitative comparison between WT and the mutants can be made from the upper panels of Figures 2 and 3.

NMR Spectral Perturbations: Backbone Amides. To assess whether the conformational change is of global nature, we performed {^1H, ^{15}N} HMQC experiments for both free (Figure 5A) and complexed (Figure 5B) forms, using uniformly ^{15}N-labeled enzymes. The cross-peaks in the spectra arise from backbone as well as side-chain $^{15}N-^1H$. Since the backbone resonances of WT·$MgAP_5A$ have been nearly completely assigned (Byeon et al., 1993), the assignment of the HMQC spectrum of K21R·$MgAP_5A$ has been

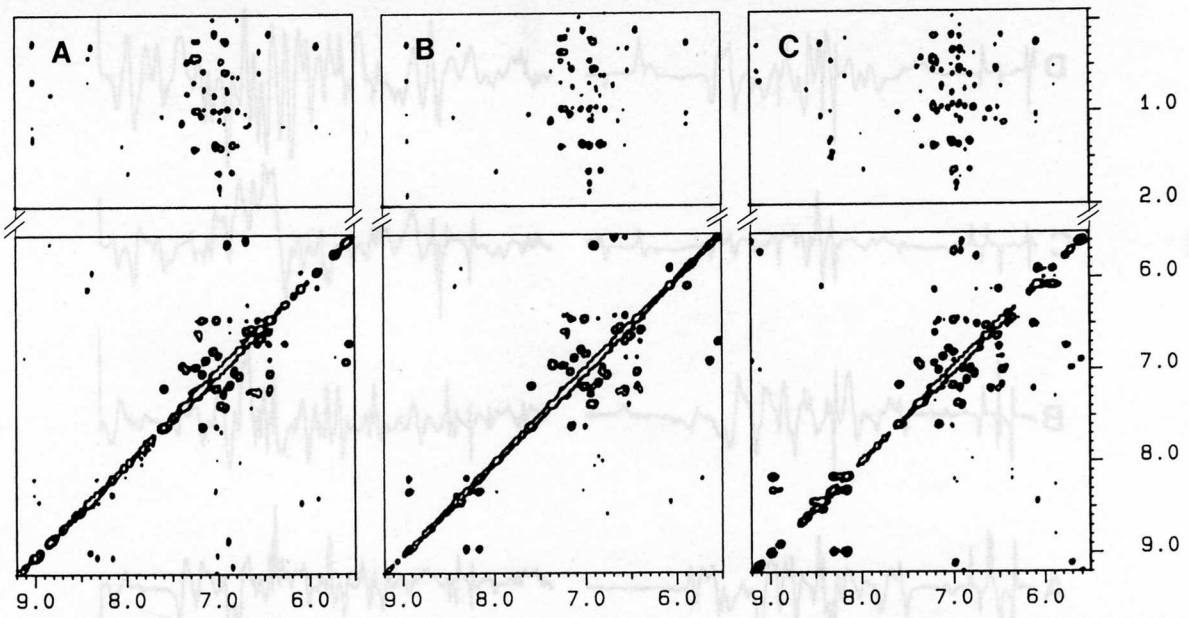

FIGURE 3: NOESY spectra of AK·MgAP$_5$A complexes with a mixing time of 120 ms: (A) WT·MgAP$_5$A; (B) K21R·MgAP$_5$A; (C) K21A·MgAP$_5$A. The same NMR samples as for Figure 1 were used.

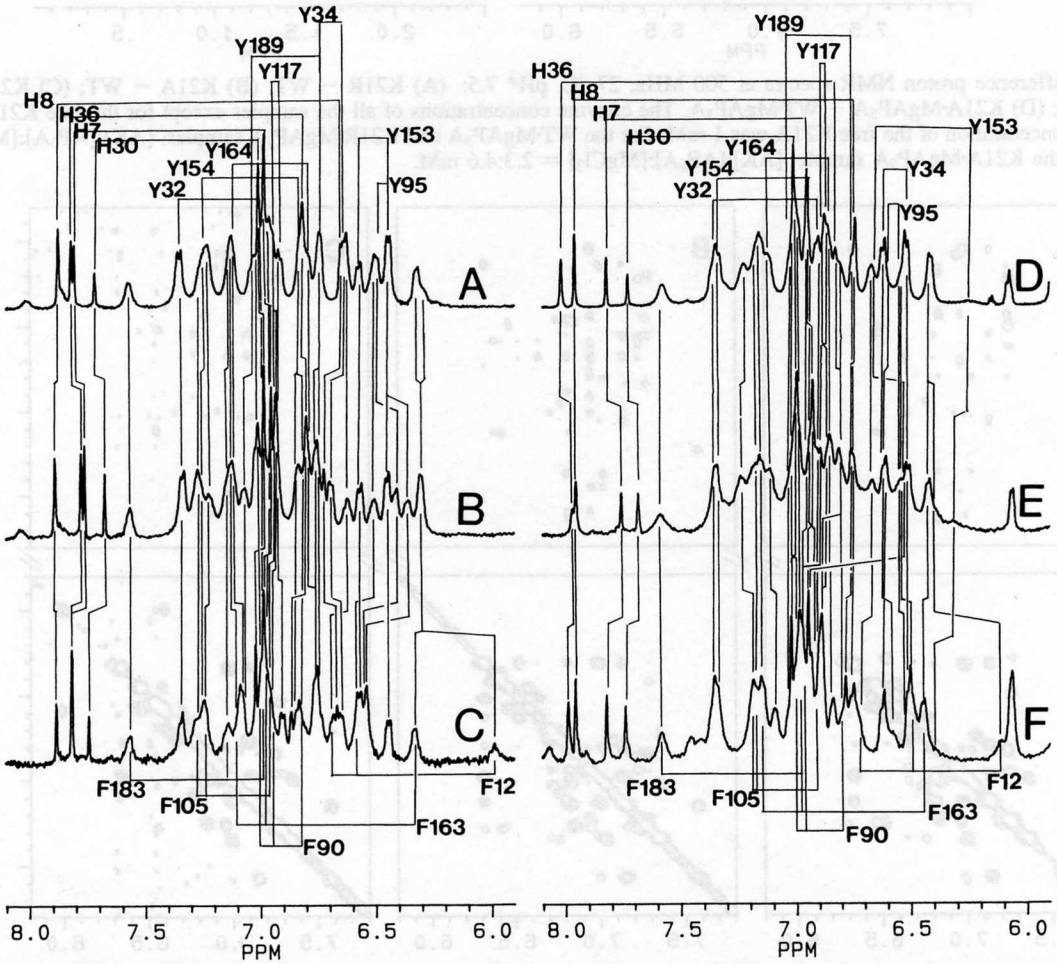

FIGURE 4: 1D proton NMR spectra showing aromatic resonance assignments of AK: (A) WT; (B) K21R; (C) K21A; (D) WT·MgAP$_5$A; (E) K21R·MgAP$_5$A; (F) K21A·MgAP$_5$A. The experimental conditions are the same as for Figure 1.

undertaken by comparison with the WT counterpart. Most of the HMQC cross-peaks in the mutant are observed at chemical shifts similar to those for WT. Similar NOE patterns are also observed in the HMQC-NOESY spectra (not shown) of both WT and the mutant. These NOE patterns not only confirm the assignments obtained from the chemical shift comparisons but also indicate the conformational conservation in K21R. The backbone $^{15}N-^{1}H$ assignments are summarized in Table 4. The NH cross-peaks which have been shifted to a greater extent ($\Delta\delta > 0.05$ and 0.5 ppm for H^N and ^{15}N, respectively) are labeled in Figure 5B and underlined in Table 4.

Analyses of the most perturbed NMR resonances can help to identify the residues that are perturbed and also help to

Table 2: Chemical Shifts (ppm) of the Aromatic Resonances of Free AK at 27 °C and pH* 7.5[a]

	WT			K21R			K21A		
residues	H_δ	H_ϵ	H_ζ	H_δ	H_ϵ	H_ζ	H_δ	H_ϵ	H_ζ
F12	6.62	6.52	6.29	6.63	6.51	6.31	6.69 (+0.07)	6.59 (+0.07)	5.99 (−0.30)
F90	7.02	6.83	6.95	7.01	6.82	6.93	7.02	6.82	6.95
F105	7.27	7.23	6.95	7.28	7.22	6.94	7.28	7.25	6.96
F163	6.33	6.98	7.13	6.31	6.98	7.12	6.33	6.98	7.10 (−0.03)
F183	7.58	7.14	7.00	7.57	7.15	7.00	7.57	7.15	6.99
Y32	7.35	7.00		7.34	7.02		7.35	6.99	
Y34	6.75	6.63		6.75	6.70 (+0.07)		6.74	6.65	
Y95	6.50	6.45		6.42 (−0.08)	6.37 (−0.08)		6.55 (+0.05)	6.53 (+0.08)	
Y117	6.95	6.92		6.94	6.92		6.99 (+0.04)	6.91	
Y153	6.58	6.45		6.57	6.45		6.57	6.45	
Y154	7.24	6.83		7.26	6.84		7.25	6.84	
Y164	7.12	6.80		7.12	6.80		7.09 (−0.03)	6.76 (−0.04)	
Y189	7.04	6.75		7.07 (+0.03)	6.76		7.08 (+0.04)	6.76	
H7	6.99	7.81		6.95 (−0.04)	7.76 (−0.05)		6.99	7.82	
H8	6.65	7.88		6.73 (+0.08)	7.90		6.67	7.89	
H30	7.01	7.72		6.99	7.68 (−0.04)		7.02	7.74	
H36	6.82	7.82		6.80	7.78 (−0.04)		6.87 (+0.05)	7.82	

[a] The underlined values are the resonances that differ from WT by more than 0.02 ppm, and the magnitudes of the differences are shown in parentheses.

Table 3: Chemical Shifts (ppm) of the Aromatic Resonances of the AK·$MgAP_5A$ Complexes at 27 °C and pH* 7.5[a]

	WT·$MgAP_5A$			K21R·$MgAP_5A$			K21A·$MgAP_5A$		
residues	H_δ	H_ϵ	H_ζ	H_δ	H_ϵ	H_ζ	H_δ	H_ϵ	H_ζ
F12	6.67	6.54	6.43	6.67	6.55	6.39 (−0.04)	6.74 (+0.07)	6.49 (−0.05)	6.11 (−0.32)
F90	7.01	6.81	6.95	7.01	6.81	6.95	7.01	6.80	6.97
F105	7.19	7.23	6.93	7.20	7.25	6.94	7.18	7.19 (−0.04)	6.91
F163	6.42	7.01	7.16	6.42	7.01	7.15	6.45 (+0.03)	6.99	7.16
F183	7.58	7.15	7.01	7.59	7.16	7.00	7.59	7.15	6.99
Y32	7.36	6.91		7.36	6.90		7.37	6.90	
Y34	6.62	6.52		6.62	6.51		6.63	6.51	
Y95	6.59	6.54		6.62 (+0.03)	6.56		6.58	6.53	
Y117	6.88	6.90		6.90	6.87 (−0.03)		6.98 (+0.10)	6.90	
Y153[b]	6.66	6.24		6.52 (−0.14)	6.31 (+0.07)		6.93 (+0.29)	6.41 (+0.17)	
Y154	7.34	6.95		7.35	6.93		7.35	6.94	
Y164	7.12	6.85		7.12	6.85		7.10	6.85	
Y189	7.03	6.75		7.04	6.75		7.03	6.76	
H7	6.95	7.82		6.93	7.76 (−0.06)		6.96	7.83	
H8	6.74	7.96		6.75	7.96		6.79 (+0.05)	7.96	
H30	7.01	7.73		7.00	7.69 (−0.04)		7.03	7.74	
H36	6.83	8.02		6.81	7.97 (−0.05)		6.88 (+0.05)	8.00	

[a] The underlined values are the resonances that differ from WT by more than 0.02 ppm, and the magnitudes of the differences are shown in parentheses. [b] The Y153 aromatic ring protons appear as very broad signals.

understand their implications in catalysis. This is not possible for all side chains since only 40% of the side-chain resonances of WT·$MgAP_5A$ have been assigned (Byeon et al., 1993). On the other hand, the backbone ^{15}N and ^1H resonances have been nearly completely assigned as shown in Table 4, except for many of the residues in the flexible P-loop (Gly15−Gly22). Careful examination of Figure 5 and Table 4 indicates that most of the $^{15}N-^1H$ cross-peaks that are shifted to a greater extent arise from residues near the active site. Among these residues, Thr23 and Arg97 have been shown to be interacting with the α-phosphates of ATP and AMP, respectively (Dahnke et al., 1992; Shi et al., 1993), and the side-chain H^ϵ of Gln101 has been shown to be in proximity to the adenine ring of AMP (Byeon et al., 1993; Müller & Schulz, 1992). It is particularly interesting that the cross-peaks for Asp140 and Asp141 experience large perturbation since these residues are conserved in all types of AK (Schulz, 1987) and have been shown to assist the catalysis by forming salt bridges with Arg138 and Arg132, respectively (Müller & Schulz, 1992; Dahnke & Tsai, 1994). The two arginine residues, whose backbone $^{15}N-^1H$ cross-peaks also shift significantly, have been shown to be critically important in stabilizing the transition state during catalysis (Yan et al., 1990a; Dahnke et al., 1992). These results suggest that the perturbations in the backbone conformation of K21R·$MgAP_5A$ are mainly localized at the active site and its immediate surrounding.

The Most Shifted Aromatic Residue in the Mutant·MgAP5A Complex: Tyr153. As shown in Table 3, the resonances of Tyr153 have been perturbed the most among the aromatic resonances. Tyr153 has not been suggested to interact with substrates directly on the basis of crystal structures. However, it is possible that this residue is involved in, or is sensitive to, substrate-induced conformational changes for three reasons: (i) This residue, conserved in all types of AK without exception (Schulz, 1987), is located right behind the P-loop. Examination of the crystal structures (Dreusicke et al., 1988; Müller & Schulz, 1992) suggested that several close contact points are observed between the Tyr153 aromatic ring and the backbones of Gly15 and Gly16. (ii) When the free WT AK binds $MgAP_5A$, the aromatic resonances of Tyr153 undergo the largest changes among all of the aromatic resonances (Tables 2 and 3). (iii) Tyr153 seems to experience quite different local motions when AK

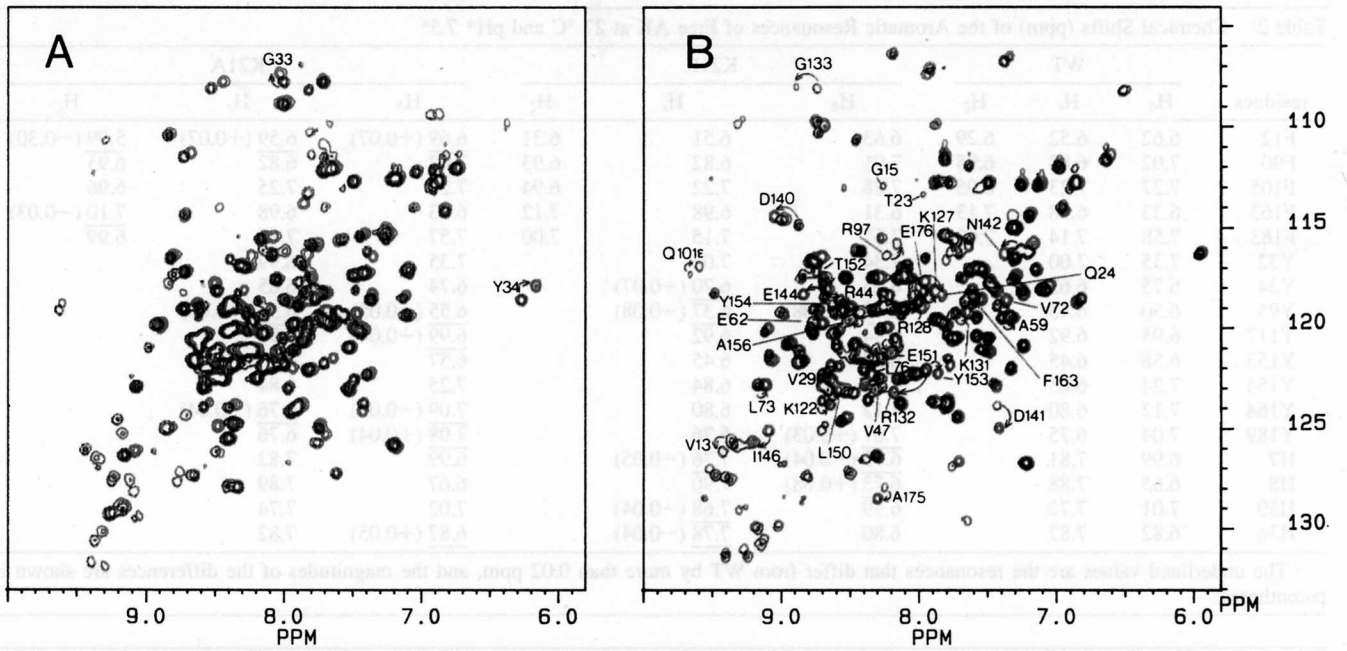

FIGURE 5: {^{1}H, ^{15}N} HMQC spectral perturbations by the K21R mutation at 500 MHz, 27 °C, pH 7.1. (A) HMQC spectrum of free K21R (red) superimposed on that of free WT (black); (B) HMQC spectrum of K21R·MgAP$_5$A (red) superimposed on that of WT·MgAP$_5$A (black). The cross-peaks which shift to a greater extent ($\Delta\delta$ > 0.05 ppm for H^N or 0.5 ppm for ^{15}N) are labeled in (B). Arrows indicate mutation-induced shifts.

is complexed to MgAP$_5$A: as shown in Figure 4, the corresponding NMR signals are detected as broad signals in the complexed form whereas they are detected as signals with reasonably narrow line width in the free form.

Since the structural and functional roles of Tyr153 have not been addressed previously by site-directed mutagenesis, we further examined this problem by constructing the mutants Y153F and Y153L. As shown in Table 1, the kinetic constants of Y153F are little perturbed relative to those of WT, whereas those of Y153L are significantly perturbed, particularly in K_m values. The increases in $K_{(MgATP)}$ and $K_{(AMP)}$ are consistent with a perturbation in substrate-induced conformational changes, and thus the role of Tyr153 in this process. The conformation of Y153L was not analyzed by NMR due to its instability, whereas the conformation of Y153F is little perturbed on the basis of 2D NOESY spectra of the MgAP$_5$A complexes (not shown). The results of Y153F suggest that the role of Tyr153 does not lie in the OH group.

Thus the majority of the residues undergoing larger changes (though small in the absolute scale) in chemical shifts are located near the substrate binding site or are possibly involved in conformational changes. The global conformation of the mutants should be relatively unchanged relative to WT in the MgAP$_5$A complexes.

^{1}H Chemical Shifts of Bound MgAP$_5$A. Having addressed the NMR properties of the proteins, we turned our attention to the bound inhibitor. The proton resonances of the two adenosine moieties of MgAP$_5$A bound to the mutants were assigned according to the procedure for WT (Yan et al., 1990a,b). The results, as summarized in Table 5, indicate that the adenine ring protons H$_2$ and H$_8$ and the ribose proton H$_{1'}$ all resonate within 0.1 ppm (except 0.16 ppm in one case) relative to the corresponding chemical shifts of the WT complex.

^{31}P NMR Analysis of WT·MgAP$_5$A. The crystal structure of *E. coli* AK·MgAP$_5$A indicates that the side chain of Lys21 forms hydrogen bonds with the second and third phosphates of the ATP moiety of AP$_5$A (Müller & Schulz, 1992), and the results of kinetic analysis of site-specific mutants indicate the importance of such interactions. However, these structural and functional analyses do not provide a critical piece of information regarding "how" the interaction between the side chain of Lys21 and the phosphate groups contributes to catalysis. This question was analyzed by 2D ^{31}P NMR of the MgAP$_5$A complexes of AK and its mutants.

The ^{31}P NMR spectra of AK·AP$_5$A and AK·MgAP$_5$A have been reported previously (Nageswara Rao & Cohn, 1977; Yan & Tsai, 1991) but not the assignments. The feature of the five phosphorus resonances from AP$_5$A changes from two clusters of signals to five unique resonances upon binding of Mg^{2+}, as shown in panels A and D of Figure 6. Such changes in chemical shifts should be due to orientation of the phosphates at specific conformations instead of purely electrostatic effects, since Mg^{2+} is able to bind to the D93A·AP$_5$A complex but unable to induce such chemical shift changes (Yan & Tsai, 1991).

To assign the resonances, we performed ^{31}P–^{31}P COSY experiments on both AK·AP$_5$A and AK·MgAP$_5$A (Figure 6). The through-bond connectivity allowed identification of the five resonances as a-e in both spectra. In principle, resonances a–e in the Mg^{2+}-free complex AK·AP$_5$A do not necessarily correspond to resonances a-e of AK·MgAP$_5$A in the same order. However, since the chemical shifts of a, d, and e are very similar between the two complexes, it is reasonable to conclude that they represent the same phosphates.

The remaining question is whether the order a–e starts from the ATP end or the AMP end. Starting from the ATP end will lead to a 2.8 ppm downfield shift and a 1.8 ppm upfield shift for the P$_\beta$ and P$_\gamma$, respectively, of the ATP moiety upon binding of Mg^{2+}. If peaks a–e start from the AMP end, peak b (shifted 2.8 ppm downfield) will correspond to the second phosphate from AMP, and the P$_\beta$ of ATP will have little shift (peak d). We assign peaks a–e to the ^{31}P nuclei α–ϵ starting from the ATP end on the basis

Table 4: Backbone ^{15}N and H^N Assignments for Chicken Adenylate Kinase at 27 °C and pH 7.1[a]

	WT·MgAP$_5$A		K21R·MgAP$_5$A			WT·MgAP$_5$A		K21R·MgAP$_5$A			WT·MgAP$_5$A		K21R·MgAP$_5$A	
	^{15}N	H^N	^{15}N	H^N		^{15}N	H^N	^{15}N	H^N		^{15}N	H^N	^{15}N	H^N
S1					L66	119.2	8.75	119.2	8.71	L130	121.3	8.85	121.8	8.86
T2					V67	123.3	8.50	123.2	8.52?	K131	119.4	7.72	119.3	7.63
E3					P68					R132	122.3	7.92	123.3	8.16
K4	117.1	7.55	117.1	7.55	L69	126.4	8.29	126.5	8.28	G133	108.1	8.72	108.1	8.87
L5	116.4	7.70	116.4	7.68	D70	116.8	8.77	116.7	8.75	E134	120.5	7.78	120.7	7.74
K6	116.5	7.28	116.7	7.27	T71	114.5	7.18	114.4	7.16	T135	107.1	7.79	106.7	7.80
H7					V72	119.0	7.41	118.7	7.34	S136				
H8	121.2	7.53	121.2	7.52	L73	122.9	9.16	122.9	9.10	G137				
K9	121.7	8.82	121.8	8.84?	D74	119.6	7.86	119.7	7.84	R138	117.8	7.46		
I10	125.0	8.67	125.2	8.70	M75	117.7	7.28	117.5	7.27	V139	123.5	8.87		
I11	130.1	9.17	130.1	9.15	L76	122.2	8.38	122.4	8.32	D140	114.9	8.86	114.5	9.03
F12	126.7	8.40	126.6	8.37	R77	120.9	8.95	120.9	8.91	D141	124.0	7.41	125.1	7.40
V13	125.7	9.35	126.3	9.41	D78	118.8	7.99	118.9	7.98	N142	116.3	7.24	116.4	7.36
V14	127.6	8.78	127.5	8.80	A79	123.8	7.76	123.9	7.79	E143				
G15	113.0	8.24			M80	117.6	8.32	117.6	8.28	E144	118.6	8.67	118.4	8.82
G16					L81	119.3	8.54			T145	119.1	8.18	119.1	8.19
P17					A82	120.6	7.70	120.7	7.72	I146	125.2	9.08	125.8	9.19
G18					K83	115.1	7.26	115.1	7.28	K147	118.4	7.61	118.2	7.59
S19					A84	124.6	7.70	124.5	7.69	K148	120.6	7.46	120.6	7.48
G20					D85					R149	121.4	9.08	121.7	9.05
K21	121.1	8.29			T86					L150	123.2	8.64	123.2	8.56
G22	107.5	7.47			S87					E151	120.7	8.15	121.3	8.18
T23	113.4	7.95			K88					T152	117.4	8.73	118.2	8.65?
Q24	117.9	8.00	118.5	7.81	G89	110.7	8.43	110.8	8.44	Y153	122.3	7.94	122.4	7.84
C25	117.9	8.68	117.6	8.68	F90	119.3	8.99	119.4	8.97	Y154	119.0	8.61	118.7	8.55
E26	119.4	8.11	121.4	8.36?	L91	125.8	9.33	125.9	9.30	K155	117.5	8.08	117.6	8.06
K27	118.7	6.80	118.8	6.83	I92	127.2	9.51	127.4	9.46	A156	119.3	8.41	119.7	8.48
I28	122.0	8.57	122.0	8.62	D93	129.3	9.06			T157	115.6	7.61	116.0	7.62
V29	123.0	8.69	122.7	8.61	G94	112.8	8.55	113.1	8.52	E158	124.1	7.79	123.9	7.77
H30	118.1	7.44	118.2	7.42	Y95	122.9	7.44	123.0	7.41	P159				
K31	117.2	7.61	117.3	7.60	P96					V160	117.6	8.13	117.6	8.09
Y32	114.7	8.98	114.7	8.96	R97	116.5	8.21	115.9	8.14	I161	119.6	7.56	119.6	7.56
G33	106.4	8.17	106.4	8.17	E98	112.1	6.95	111.9	6.96	A162	120.9	7.22	121.0	7.21
Y34	116.4	5.94	116.4	5.92	V99	128.6	9.55	128.6	9.54	F163	118.8	7.65	118.7	7.57
T35	117.5	8.82	117.6	8.84	K100	120.3	9.10	120.1	9.08	Y164	115.7	7.72	115.8	7.70
H36	131.5	9.39	131.5	9.39	Q101	114.1	6.94	114.3	6.92	K165	124.8	8.54	124.6	8.51
L37	130.7	9.10	130.9	9.13	G102	112.8	7.77	112.9	7.75	G166	112.1	6.71?		
S38	119.4	8.58	119.3	8.60	E103	122.6	8.09	122.6	8.13	R167	121.6	8.45		
T39					E104	117.6	8.51	117.6	8.52	G168				
G40					F105	119.9	7.80	120.0	7.77	I169	108.2	6.49	108.3	6.47
D41	123.3	7.79			E106	119.3	8.32	119.2	8.28	V170	123.7	8.35	123.7	8.35
L42	123.3	8.46	122.9	8.48	K107	117.1	7.51	117.2	7.51	R171	129.9	8.99	129.9	9.00
L43	121.5	8.35			K108	115.5	7.79	115.5	7.78	Q172	126.9	8.99	126.8	8.96
R44	119.3	8.54	119.1	8.48	I109	121.4	8.41	121.6	8.42	L173	129.0	9.25	129.2	9.29
A45	123.9	8.12	123.9	8.11	A110	122.1	7.31	122.2	7.31	N174	121.9	9.08	121.7	9.07
E46	121.2	7.50	121.3	7.46	P111					A175	128.0	8.23	128.6	8.28
V47	122.6	8.27	123.2	8.30	P112					E176	118.5	8.03	117.8	7.94
S48	116.3	8.40	116.2	8.44	T113	118.4	9.48	118.4	9.47	G177	106.8	7.36	106.6	7.32
S49	117.6	7.69	117.6	7.66	L114	117.8	7.46	117.9	7.47	T178	110.4	8.71	110.1	8.67
G50	110.0	7.87	110.0	7.85	L115	127.3	8.50	127.4	8.48	V179	120.3	8.60	120.2	8.56
S51	116.6	7.93	116.6	7.94	L116	127.5	9.39	127.7	9.36	D180	117.5	8.08	117.6	8.09
E52					Y117	128.9	8.83	128.6	8.82	E181	123.7	7.89	123.8	7.86
R53					V118	131.2	9.26	131.5	9.23	V182	122.3	8.64	122.5	8.68
G54	109.8	8.72	109.9	8.73	D119	127.1	7.74	126.8	7.69	F183	121.6	8.45	121.6	8.40?
K55	122.4	8.03	122.4	8.00	A120	129.7	7.67	129.7	7.62	Q184	120.1	8.26	120.1	8.21?
K56	120.5	7.56	120.5	7.55	G121	109.9	9.30	109.7	9.27	Q185	119.5	7.30	119.6	7.32
L57	119.2	8.09	119.2	8.10	K122	123.7	8.69	123.9	8.63	V186	121.6	8.26	121.7	8.31
Q58	121.0	8.44	120.9	8.44	E123	116.8	8.73	116.6	8.69	C187	118.4	8.25	118.4	8.23
A59	119.6	7.38	119.6	7.30	T124	118.6	7.57	118.7	7.53	S188	115.1	7.30	115.1	7.30
I60	118.2	7.23	118.4	7.22	M125	121.6	7.77	122.0	7.75	Y189	118.2	7.08	118.1	7.08
M61	119.0	8.24	119.0	8.23	V126	117.0	8.06	117.1	8.10	L190	121.0	8.58	120.9	8.58
E62	120.1	8.77	119.9	8.68	K127	118.3	7.95	118.3	7.86	D191	120.3	8.75	120.4	8.75
K63	116.3	7.18	115.9	7.15	R128	118.5	8.20	119.0	7.96	K192	117.1	7.13	117.2	7.12
G64	107.1	7.90	107.5	7.92	L129	121.1	8.13	121.3	8.18?	L193	126.9	7.20	126.9	7.19
E65	118.2	7.06	118.1	7.03										

[a] Proton chemical shifts are ±0.01 ppm. The nitrogen shifts are ±0.1 ppm. The resonances which shift to a greater extent ($\Delta\delta$ > 0.05 and 0.5 ppm for H^N and ^{15}N, respectively) are underlined. The nitrogen shifts listed here are 1.6 ppm smaller than those reported in Byeon et al. (1993). The discrepancy arises from using different references: the previous work was referenced using 2.9 M $^{15}NH_4Cl$ in 1 M HCl, while this work uses 1.5 M $^{15}NH_4NO_3$ in 1 M HNO_3. We changed the reference to the latter because ammonium nitrate is a better reference since its chemical shift does not vary with pH and concentration (Srinvasan & Lichter, 1977). Question marks indicate that the assignments are uncertain or tentative.

of the following reasons: (i) Although it has been cautioned that one should be careful in equating the chemical shift changes to the sites of coordination (Jeffe & Cohn, 1978; Huang & Tsai, 1982) because the chemical shifts of ^{31}P

Table 5: Chemical Shifts (ppm) of Nucleotide Protons in AK·$MgAP_5A$ Complexes at 27 °C and pH* 7.5[a]

complex	H_2			H_8			$H_{1'}$		
WTAK·$MgAP_5A$[b]	9.00 (I)	8.31 (II)	8.14 (f)	8.36 (I)	8.41 (II)	8.41 (f)	5.90 (I)	6.07 (II)	6.08 (f)
K21R·$MgAP_5A$[c]	8.92 (I)	8.30 (II)	8.15 (f)	8.35 (I)	8.41 (II)	8.41 (f)	5.87 (I)	6.06 (II)	6.06 (f)
K21A·$MgAP_5A$[d]	8.97 (I)	8.31 (II)	8.16 (f)	8.52 (I)	8.42 (II)	8.42 (f)	5.90 (I)	6.07 (II)	6.07 (f)

[a] Sites I and II represent the AMP and MgATP moieties of $MgAP_5A$, respectively; f denotes a free state arising from excess AP_5A. [b] 2.0 mM WT + 2.4 mM AP_5A + 4.6 mM $MgCl_2$. [c] 2.0 mM K21R + 2.4 mM AP_5A + 4.6 mM $MgCl_2$. [d] 2.0 mM K21A + 3.0 mM AP_5A + 4.6 mM $MgCl_2$.

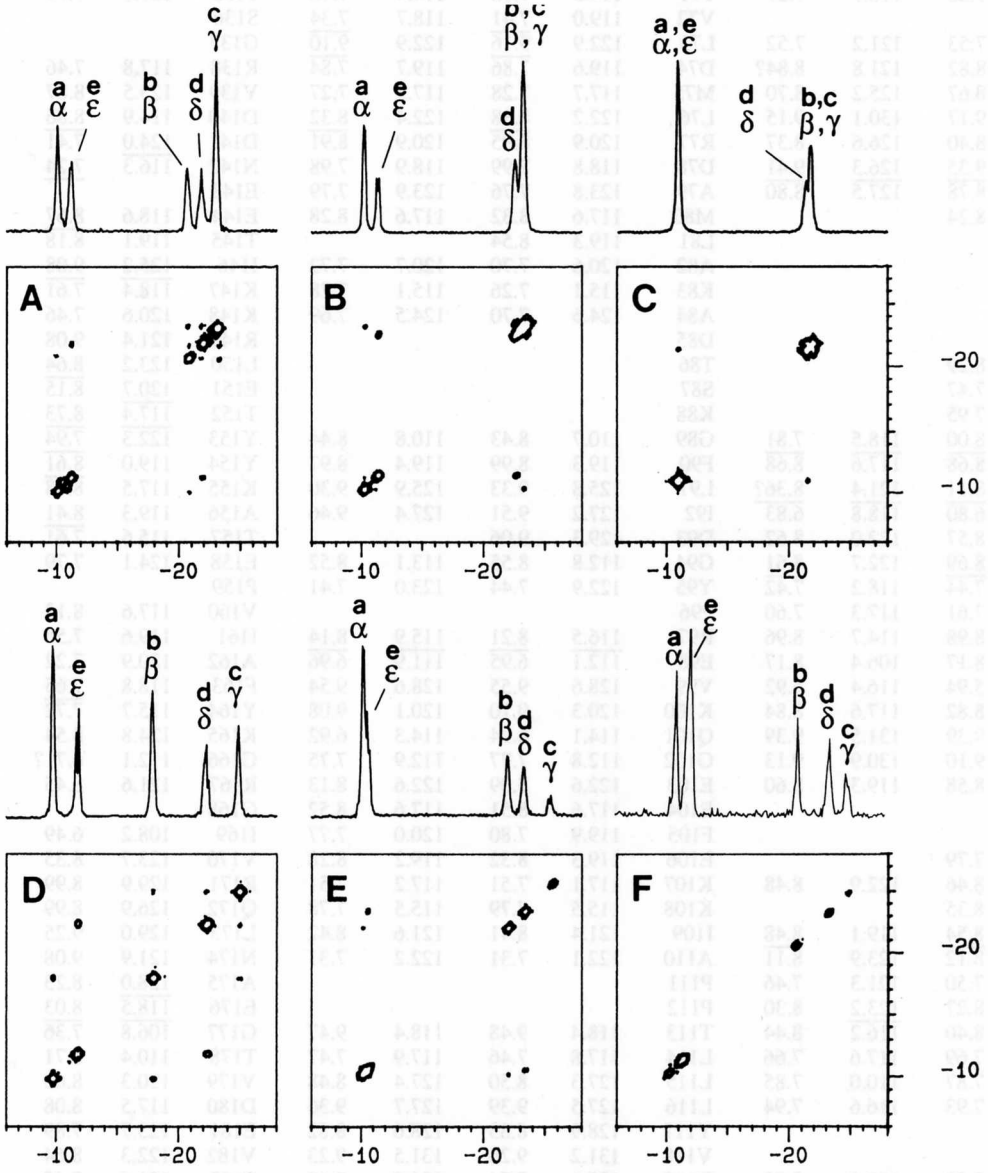

FIGURE 6: 2D $^{31}P-^{31}P$ COSY spectra of various AP_5A complexes at 121.4 MHz, 25 °C, pH 7.8: (A) WT·AP_5A; (B) K21R·AP_5A; (C) K21A·AP_5A; (D) WT·$MgAP_5A$; (E) K21R·$MgAP_5A$; (F) K21A·$MgAP_5A$. [AK]:[AP_5A] = 1:0.9 mM for (A)−(C) and [AK]:[AP_5A]:[$MgCl_2$] = 1:0.9:2 mM for (D)−(F). The 1D spectra on the top of each 2D spectra are the projections of 2D COSY spectra into the f_2 dimension.

nuclei are sensitive to bond lengths and bond angles (Gorenstein,1981), the pattern of changes upon binding of Mg^{2+} is best interpreted to suggest that peaks b and c correspond to the sites of coordination. (ii) It has been well-established that Mg^{2+} does not bind to the substrate at the AMP site (AMP or ADP) in the resting state (Nageswara Rao et al., 1978). (iii) The results of stereochemical studies have suggested that the mode of coordination of MgATP as a substrate of AK is β,γ-bidentate (Dunaway-Mariano & Cleland, 1980; Tomasselli & Noda,1983; Kalbitzer et al., 1983), even though the coordination to P_γ has not been demonstrated spectroscopically (Kalbitzer et al., 1983). (iv) The large downfield shift of peak b upon binding of Mg^{2+} is consistent with the downfield shift of the P_β resonance of AK·ATP upon binding of Mg^{2+} established previously (Nageswara Rao et al., 1978; Shyy, 1987).

Changes in the ^{31}P NMR Properties of the Mutants. The next step is to examine the effects of Lys21 mutation on the ^{31}P resonances. The $^{31}P-^{31}P$ COSY spectra of K21R·AP_5A and K21R·$MgAP_5A$ are shown in panels B and E of Figure 6, respectively, and the corresponding spectra for the complexes of the K21A mutant are shown in panels C and F of Figure 6, respectively. The assignments of the ^{31}P resonances were made from the COSY spectra as described for WT. The results of assignments are summarized in Table 6. Figure 6 indicates that the ^{31}P resonances are similar

Table 6: ^{31}P Chemical Shifts (ppm) of AP_5A in AP_5A or $MgAP_5A$ Complexes of AK at 25 °C and pH 7.8

	δ in AP_5A complexes[a]					$\Delta\delta$ in $MgAP_5A$ complexes[b]				
	α	β	γ	δ	ϵ	α	β	γ	δ	ϵ
WT	−10.2	−20.7	−23.1	−21.9	−11.3	+0.4	+2.8	−1.8	−0.4	−0.5
K21R	−10.3	−23.3	−23.3	−22.6	−11.5	+0.1	+1.3	−2.1	−0.7	+0.8
K21A	−11.0	−21.8	−21.8	−21.4	−11.0	+0.7	+1.2	−2.9	−1.7	−0.3

[a] Chemical shifts (δ) are listed for the AP_5A complexes ([AK]:[AP_5A] = 1:0.9 mM). [b] On the other hand, $\Delta\delta$, the chemical shift differences ($\delta_{AK\cdot MgAP_5A} - \delta_{AK\cdot AP_5A}$), are listed for the $MgAP_5A$ complexes ([AK]:[AP_5A]:[$MgCl_2$] = 1:0.9:2 mM).

between WT and the mutants in the Mg^{2+}-free complexes, but they become significantly different in the presence of Mg^{2+}. The largest perturbation in the complex forms is observed for P_β (−4.1 ppm for K21R and −2.7 ppm for K21A).

The fact that K21A and K21R have similar ^{31}P NMR properties suggests that the differences in the ^{31}P chemical shifts between WT and the mutants are not caused purely by electrostatic effect or steric effect. Instead, the side chain of Lys21 must be involved in a very precise orientation of the polyphosphate chain of $MgAP_5A$, which is a well-established bisubstrate analog of AK. The conservative arginine is unable to substitute for lysine for this orientational function. Furthermore, the side chain of Lys21 and Mg^{2+} appear to function cooperatively. In the WT AK the magnesium cation binds to the phosphates and orients the phosphate chain to a proper conformation while in K21R or K21A the cation is unable to orient the phosphate chain properly.

DISCUSSION

Possible Functional Roles of Lys21. Although the way Lys21 interacts with the substrate MgATP of muscle AK can now be clearly deduced from the crystal structure of *E. coli* AK·$MgAP_5A$ (Müller & Schulz, 1992) and *E. coli* AK·AMP·AMPPNP (Berry et al., 1994), our work started when the high-resolution crystal structure was not yet available (Tian et al., 1990). The results presented in this paper have led to the following conclusions independent of the crystal structure: (i) The side chain of Lys21 stabilizes the transition state in the catalysis of AK by up to 7 kcal/mol, since the ratio k_{cat}/K_m of mutants decreases by a factor of ca. 10^5. This quantitative interpretation has been reached after showing that the perturbations in the conformation of the mutants are mainly localized at active site residues and Tyr153. The importance of Lys21 in catalysis supports the hypothesis by Reinstein et al. (1990) that this lysine stabilizes the transition state. (ii) Lys21 functions by orienting the triphosphate chain of MgATP to a proper conformation required for catalysis, as suggested by ^{31}P NMR analyses. (iii) The interaction between Lys21 and the phosphate chain in turn affects the interactions between the substrates and the active site residues. In the K21R·MgATP complex, the NH chemical shifts of many of the active site residues are perturbed. Thus the 7 kcal/mol contribution should be considered a maximal value for Lys21 alone; it could include partial contributions by the residues which function cooperatively with Lys21. (iv) The catalytic functions of Lys21 cannot be replaced by a conservative residue arginine. In addition, since K21A and K21R behave similarly, the catalytic function of Lys21 should not be merely a charge effect. Thus our results have not only demonstrated that Lys21 joins with three arginine residues (132, 138, and 149) as the most critical residues in stabilizing the transition state of AK catalysis (Tsai & Yan, 1991) but also provided detailed functional roles of Lys21 at the structural level.

How Can the Problem of Conformational Perturbations Be Overcome? The first of our four conclusions could have been reached 4 years ago from the kinetic data of K21M (Tian et al., 1990). However, the large perturbation in the 1D proton NMR spectrum led us to conclude that Lys21 plays a structural role, possibly by stabilizing the P-loop, and that its functional role remains to be established. Why did it take 4 years to determine the functional role? Once the structure of a mutant has been shown to be perturbed, one is faced with a difficult dilemma: the structure of the mutant enzyme needs to be determined for comparison with that of WT, which is a major endeavour in the case of AK. However, even if this can be achieved, one still cannot attribute a specific structural change to a specific functional change, even though this is a common practice by structural biologists.

We have not determined the tertiary structures of WT or mutants. However, we have assigned most of the backbone resonances and ca. 40% of the side-chain resonances of AK·$MgAP_5A$ and have identified the residues in proximity to the adenosine moieties (Byeon et al., 1993). The assignment information has allowed us to identify the residues whose N−H resonances experience greater perturbations, which is a useful but not commonly used approach to monitor structural perturbation. Although this method cannot detect conformational changes in side chains, it can nicely detect global changes in the backbone. Our analyses suggest that structural perturbations are mainly localized near the active site, which then led us to conclude that the conformational perturbations in the mutants are more likely to be local than global. Such structural analyses can only ease the concern about structural perturbations in the mutants. Further confidence in the conclusion has been gained from the results of NMR analyses of bound AP_5A: the resonances of the two adenosine moieties (Table 5) and the two terminal phosphates (Table 6) are not significantly perturbed. Overall, the effect of Lys21 in catalysis appears to be "site-specific".

Possible Structural Roles of Lys21. The conformations of the free enzymes have been analyzed in less detail since the total assignment of free WT AK has not yet been accomplished. However, all of the aromatic and some of the $^{15}N-^{1}H$ resonances of free AK were assigned by comparing its NOE cross-peaks and the chemical shifts with those for the complexed form. It is interesting to note that the Lys21 mutations perturb somewhat different residues between the free and the complexed forms. For example, Tyr34 experiences a large perturbation in the free form but little shift in the complexed form (Figure 5), while Tyr153 behaves just oppositely (Tables 2 and 3). This observation alludes to the importance of analyzing the conformations of the substrate or inhibitor complexes, not just the free enzymes. We might not have reached the same conclusion

had we only analyzed the NMR properties of the free enzymes. By examining the crystal structure of the 2.1 Å crystal structure of porcine muscle AK (Dreusicke et al., 1988), we believe that Lys21 indeed also plays a structural role by stabilizing the P-loop in the free enzyme, as we have interpreted previously (Tian et al., 1990). As indicated by Dreusicke and Schulz (1986), the distances between the side-chain nitrogen atom of Lys21 and the carbonyl oxygen atoms of Gly15 and Gly16, which are in the opposite side of the loop, are 2.8 and 3.3 Å, respectively. They may form hydrogen bonds to stabilize the P-loop. The same hydrogen bonds may also exist in the complexed form because an analysis of the crystal structure of *E. coli* AK·$MgAP_5A$ (Müller & Schulz, 1992) shows that the corresponding distances are both 3.1 Å. The fact that the backbone N−H cross-peaks of Gly15, Lys21, Gly22, and Thr23 disappear (or shift too extensively to follow) in the $MgAP_5A$-complexed K21R (Figure 5 and Table 5) is consistent with disruption of these hydrogen bonds.

Conclusion. Although the "essential lysine" is obviously important for catalysis, it has been difficult to demonstrate experimentally. However, using K21R and K21A mutants, we have again demonstrated that site-directed mutagenesis, in conjunction with detailed structural and functional analyses, can uncover structural and functional roles of a specific residue far beyond what can be obtained by crystal structures or by straightforward analyses of kinetic data. The essential lysine plays several important structural and functional roles: it stabilizes the P-loop, orients the triphosphate chain of ATP to proper conformations, and ensures proper interactions between the substrates and the active site residues and the magnesium ion. A conserved mutation to Arg is sufficient to cause localized conformational changes, disrupt the conformation of the polyphosphate chain of AP_5A, perturb the interaction of AP_5A with Mg^{2+} and several active site residues, and cause k_{cat}/K_m to decrease by a factor of 10^5.

ACKNOWLEDGMENT

The authors thank Dr. C. E. Cottrell for his assistance in setting up $^{31}P-^{31}P$ COSY and $\{^1H,^{15}N\}$ HMQC-NOESY experiments.

REFERENCES

Berry, M. B., Meador, B., Bilderback, T., Liang, P., Glaser, M., & Phillips, G. N., Jr. (1994) *Proteins 19*, 183−198.
Bodenhausen, G., Kogler, H., & Ernst, R. R. (1984) *J. Magn. Reson. 58*, 370−388.
Byeon, I.-J. L., Yan, H., Edison, A. S., Mooberry, E. S., Abildgaard, F., Markley, J. L., & Tsai, M.-D. (1993) *Biochemistry 32*, 12508−12521.
Cleland, W. W. (1986) in *Investigation of Rates and Mechanisms of Reactions Part 1* (Bernasconi, C. F., Ed.) pp 791−870, John Wiley and Sons, New York.
Dahnke, T., & Tsai, M.-D. (1994) *J. Biol. Chem. 269*, 8075−8081.
Dahnke, T., Shi, Z., Yan, H., Jiang, R.-T., & Tsai, M.-D. (1992) *Biochemistry 31*, 6318−6328.
Dreusicke, D., & Schulz, G. E. (1986) *FEBS Lett. 208, 301*−304.
Dreusicke, D., Kauplus, P. A., & Schulz, G. E. (1988) *J. Mol. Biol. 199*, 359−371.
Dunaway-Mariano, D., & Cleland, W. W. (1980) *Biochemistry 19*, 1506−1515.
Gorenstein, D. G. (1981) *Annu. Rev. Biophys. Bioeng. 10*, 355−386.
Huang, S. L., & Tsai, M.-D. (1982) *Biochemistry 21*, 951−959.
Jaffe, E. K., & Cohn, M. (1978) *Biochemistry 17*, 652−657.
Kalbitzer, H. R., Marquetant, R., Connolly, B. A., & Goody, R. S. (1983) *Eur. J. Biochem. 133*, 221−227.
Kishi, F., Maruyama, M., Tanizawa, Y., & Nakazawa, A. (1986) *J. Biol. Chem. 261*, 2942−2945.
Marion, D., & Wüthrich, K. (1983) *Biochem. Biophys. Res. Commun. 113*, 967−974.
Mueller, L. (1979) *J. Am. Chem. Soc. 101*, 4481−4484.
Müller, C. W., & Schulz, G. E. (1992) *J. Mol. Biol. 224*, 159−177.
Nageswara Rao, B. D., & Cohn, M. (1977) *Proc. Natl. Acad. Sci. U.S.A. 74*, 5355−5357.
Nageswara Rao, B. D., Cohn, M., & Noda, L. (1978) *J. Biol. Chem. 253*, 1149−1158.
Reinstein, J., Schlichting, I., & Wittinghofer, A. (1990) *Biochemistry 29*, 7451−7459.
Rhoads, D. G., & Lowenstein, J. M. (1968) *J. Biol. Chem. 243*, 3963−3972.
Saraste, M., Sibbald, P. R., & Wittinghofer, A. (1990) *Trends Biochem. Sci. 15*, 430−434.
Schulz, G. E. (1987) *Cold Spring Harbor Symp. Quant. Biol. 52*, 429−439.
Schulz, G. E., Schiltz, E., Tomasselli, A. G., Frank, R., Brune, M., Wittinghofer, A., & Schirmer, R. H. (1986) *Eur. J. Biochem. 161*, 127−132.
Shaka, A. J., Keeler, J., Frenkiel, T. A., & Freeman, R. (1983) *J. Magn. Reson. 52*, 335−338.
Shaka, A. J., Barker, P. B., & Freeman, R. (1985) *J. Magn. Reson. 64*, 547−552.
Shi, Z, Byeon, I.-J. L., Jiang, R.-T., & Tsai, M.-D. (1993) *Biochemistry 32*, 6450−6458.
Shyy, Y.-J. (1987) Ph.D. Dissertation, The Ohio State University, pp 157−160.
Srinvasan P. R., & Lichter R. L. (1977) *J. Magn. Reson. 28*, 227−234.
Tagaya, M., Yagami, T., & Fukui, T. (1987) *J. Biol. Chem. 262*, 8257−8261.
Tanizawa, Y., Kishi, F., Kaneko, T., & Nakazawa, A. (1987) *J. Biochem. (Tokyo) 101*, 1289−1296.
Tian, G., Sanders, C. R., II, Kishi, F., Nakazawa., A., & Tsai, M.-D. (1988) *Biochemistry 27*, 5544−5552.
Tian, G., Yan, H., Jiang, R.-T., Kishi, F., Nakazawa, A., & Tsai, M.-D. (1990) *Biochemistry 29*, 4296−4304.
Tomasselli, A. G., & Noda, L. H. (1983) *Eur. J. Biochem. 132*, 109−115.
Tsai, M.-D., & Yan, H. (1991) *Biochemistry 30*, 6806−6818.
Tsai, M.-D., Jiang, R.-T., Dahnke, T., & Shi, Z. (1994) *Methods Enzymol. 249*, 425−443.
Wittinghofer, A., & Pai, E. F. (1991) *Trends Biochem. Sci. 16*, 382−387.
Yagami, T., Tagaya, M., & Fukui, T. (1988) *FEBS Lett. 229*, 261−264.
Yan, H., & Tsai, M.-D. (1991) *Biochemistry 30*, 5539−5546.
Yan, H., Shi, Z., & Tsai, M.-D. (1990a) *Biochemistry 29*, 6385−6392.
Yan, H., Dahnke, T., Zhou, B., Nakazawa, A., & Tsai, M.-D. (1990b) *Biochemistry 29*, 10956−10964.

BI942144U